OFFICE OF NAVAL RESEARCH

Grant or Contract N00014-91WX24155

R&T Code 4134053

Technical Report No. 1

Growth of Near-Free-Standing $YBa_2Cu_3O_7$-Type Crystals Using a Self-Decanting Flux Method

by

T. A. Vanderah, C. K. Lowe-Ma, D. E. Bliss, and M. W. Decker
Chemistry Division, Research Department
Naval Weapons Center, China Lake, CA 93555

and

M. S. Osofsky, E. F. Skelton, and M. M. Miller
Naval Research Laboratory
Washington, DC 20375-5000

Submitted for publication in
The Journal of Crystal Growth

May 1991

REPORT DOCUMENTATION PAGE

Form Approved
OMB No. 0704-0188

1. AGENCY USE ONLY *(Leave blank)*	2. REPORT DATE	3. REPORT TYPE AND DATES COVERED
	May 1991	Technical Report #1 10/90-4/91

4. TITLE AND SUBTITLE
Growth of Near-Free-Standing $YBa_2Cu_3O_7$-Type Crystals Using a Self-Decanting Flux Method

5. FUNDING NUMBERS
N00014-91WX24155

6. AUTHORS
T. A. Vanderah, C. K. Lowe-Ma, D. E. Bliss, M. S. Osofsky, E. F. Skelton, and M. M. Miller

7. PERFORMING ORGANIZATION NAME(S) AND ADDRESS(ES)
Naval Weapons Center
China Lake, CA 93555-6001

8. PERFORMING ORGANIZATION REPORT NUMBER

9. SPONSORING/MONITORING AGENCY NAMES(S) AND ADDRESS(ES)
Office of Naval Research (Chemistry Program)
800 N. Quincy Street
Arlington, VA 22217

10.. SPONSORING/MONITORING AGENCY REPORT NUMBER

11. SUPPLEMENTARY NOTES
Submitted for publication in Journal of Crystal Growth

12a. DISTRIBUTION /AVAILABILITY STATEMENT

12b. DISTRIBUTION CODE

13. ABSTRACT *(Maximum 200 words)*

Large (multi-millimeter-sized) near-free-standing platelets of $YBa_2Cu_3O_x$ have been obtained using a self-decanting flux method. The charge composition consists of 10.2 wt % $YBa_2Cu_3O_7$ in a 0.28:0.72 molar BaO:CuO flux-mixture induced to decant by a thermal gradient. After oxygen-annealing, crystals display sharp T_c values near 92 K. Crystals of ten of the $RBa_2Cu_3O_x$ congeners, R = Pr, Nd, Sm, Eu, Gd, Dy, Ho, Er, Tm, and Yb, were also grown using the method described. Preliminary experiments were successful in adapting the procedure to the $Nd_{1.85}Ce_{0.15}CuO_4$ system and yielded small, superconducting ($T_c > 20$ K) platelets after Ar-annealing. For the $YBa_2Cu_3O_x$ system, an oxygen-annealing study was conducted in order to determine the best conditions for the reliable production of crystals with optimized superconducting properties.

14. SUBJECT TERMS
Yttrium barium copper oxide, crystal growth, oxygen-annealing

15. NUMBER OF PAGES

16. PRICE CODE

17. SECURITY CLASSIFICATION OF REPORT	18. SECURITY CLASSIFICATION OF THIS PAGE	19. SECURITY CLASSIFICATION OF ABSTRACT	20. LIMITATION OF ABSTRACT
UNCLASSIFIED	UNCLASSIFIED	UNCLASSIFIED	UL

Submitted to J. Crystal Growth
5/91

Growth of Near-Free-Standing $YBa_2Cu_3O_7$-Type Crystals Using a Self-Decanting Flux Method

T.A. Vanderah, C.K. Lowe-Ma, D.E. Bliss, and M.W. Decker
Chemistry Division, Research Department
Naval Weapons Center
China Lake, CA 93555

M.S. Osofsky, E.F. Skelton, and M.M. Miller
Naval Research Laboratory
Washington, D.C. 20375-5000

ABSTRACT

Large (multi-millimeter-sized) near-free-standing platelets of $YBa_2Cu_3O_x$ have been obtained using a self-decanting flux method. The charge composition consists of 10.2 wt% $YBa_2Cu_3O_7$ in a 0.28:0.72 molar BaO:CuO flux-mixture induced to decant by a thermal gradient. After oxygen-annealing, crystals display sharp T_c values near 92 K. Crystals of ten of the $RBa_2Cu_3O_x$ congeners, R = Pr, Nd, Sm, Eu, Gd, Dy, Ho, Er, Tm, and Yb, were also grown using the method described. Preliminary experiments were successful in adapting the procedure to the $Nd_{1.85}Ce_{0.15}CuO_4$ system and yielded small, superconducting (T_c > 20 K) platelets after Ar-annealing. For the $YBa_2Cu_3O_x$ system, an oxygen-annealing study was conducted in order to determine the best conditions for the reliable production of crystals with optimized superconducting properties.

INTRODUCTION

The post-1986 explosion in research on complex cuprates found to exhibit superconductivity above the boiling point of liquid nitrogen has been accompanied by considerable efforts to grow large, high-quality single crystals of these unusual phases [1-6]. The chemical/structural nature of the superconducting cuprate systems, typified by thermodynamic instability, nonstoichiometry, and two-dimensional structures notoriously prone to defects and intergrowths, has presented crystal growers with a formidable challenge in the development of reliable procedures that yield samples with optimum properties.

To date, crystal growth of the $YBa_2Cu_3O_7$ system has been the most intensively studied [7-29]. Pertinent phase diagram studies are now available [25,30-32], and detwinning procedures have been developed [33-36] to facilitate anisotropic property-studies of superconducting orthorhombic crystals. As $YBa_2Cu_3O_7$ melts incongruently and is reactive or insoluble in many common fluxes, the number of applicable crystal growth methods is limited. Although some success has been reported using alkali halide [26,27,37] and K_2CO_3 [28] fluxes, crystals are most easily grown from BaO:CuO mixtures [10-25,29,38] at or near the eutectic composition (0.28:0.72 molar, respectively) which melts near 890°C [30].

The most popular charge composition used to grow $YBa_2Cu_3O_x$ crystals is a 1:4:10 molar mixture of $YO_{1.5}$:BaO:CuO [10,16,18,19,38], which corresponds to approximately 40 wt% $YBa_2Cu_3O_7$ in a 0.28:0.72 molar BaO:CuO solvent. This concen-

tration is not critical, however, as good superconducting crystals have also been obtained from charges corresponding to 24 [21], 18 [11], 10 [20], and 5 [23] wt% loadings of $YBa_2Cu_3O_7$ in the eutectic BaO:CuO flux. The viscosity and flow-properties of the BaO:CuO solvent result in marked creeping tendencies [20,21-23,29,39], termed by some as "superflow" [22]. At high temperatures, the liquid flux tends to wet the container sides to a greater degree than the surfaces of $YBa_2Cu_3O_7$ crystals; thus, in many experiments the flux flows away from the crystals, leaving large clean pieces that can be mechanically extracted. This phenomenom is not easily controlled, however, and the reproducible growth of large, free, clean crystals remains difficult. Some success has been reported in taking advantage of the low viscosity and wetting properties of the flux to remove it cleanly from the crystals at high temperatures by wicking with a porous ceramic piece [23], or by decanting [20,38]. If the flux does not flow away from the crystals, retrieval of intact crystals is problematic since no solvent is known that exclusively dissolves the flux.

In the present report we describe a reasonably reproducible method in which a thermal gradient across the crystal growth container, in combination with the unusual flow-properties of the BaO:CuO flux, results in near-complete self-decantation, leaving large platelets that are easily freed. The method was used to obtain multi-millimeter-sized $YBa_2Cu_3O_x$ crystals with good superconducting properties as well as millimeter-sized crystals of ten of the analogous $RBa_2Cu_3O_x$ compounds. Preliminary experiments

were also successful in adapting the procedure to grow crystals of $Nd_{1.85}Ce_{0.15}CuO_4$. Also reported here are the results of a post-growth oxygen-annealing study of $YBa_2Cu_3O_x$ crystals in which the effects of various heating profiles on the details of the superconducting transitions and the oxygen-content-sensitive [10,13,16,21] c-axis lattice parameters were examined.

CRYSTAL GROWTH PROCEDURE

$YBa_2Cu_3O_7$ crystal growth mixtures were prepared from Y_2O_3, $BaCO_3$, and CuO of 99.99% or higher purity. The corresponding rare earth sesquioxide was substituted for each of the $RBa_2Cu_3O_7$ analogs. The composition chosen was 10.2 wt% $YBa_2Cu_3O_7$ in the BaO:CuO 0.28:0.72 mol eutectic solvent, resulting in an overall molar charge composition of 1:18.4:45.1 = Y:Ba:Cu. This particular mixture, which features a relatively large concentration of solvent, was reported by Sadowski and Scheel [20] to yield thick, multimillimeter-sized $YBa_2Cu_3O_x$ crystals; similar results were reported by Wolf, et al. [39]. The components were mixed by grinding with an agate mortar and pestle for 30 min. Zirconia was chosen as the crystal growth container to minimize contamination of the crystals and degradation of superconducting properties [6,10,18,20,21,39]. The best results were obtained using round-bottom crucibles (32 mm diameter x 22 mm high) (Coors Ceramicon Designs, McDanel, Atomergic) that were packed with 25-30 g charge. Crucibles could frequently be re-used after they were thoroughly cleaned with aqua regia solution, soaked for several days in water, and dried in a vacuum oven at 150°C.

Crystal growth experiments were carried out in a small muffle furnace (Thermolyne Model F-A1315M; heating chamber 10x10x10 cm^3) using the following heating program:

1. Heat in 3.5 h to T_{max}[1]; soak 20 h.
2. Step-cool 40°C; stabilize 30 min.
3. Cool at 0.4°/h to 850°C.
4. Cool at 8-9°/h to ambient.[2]

Packed crucibles were supported on a bed of alumina powder and centered in the furnace at a distance from the door that resulted in the temperature differences shown in Figure 1 for a $YBa_2Cu_3O_7$ experiment. Self-decanting occurs during Step 3 of the program above; a "decant-fan" up to several cm long grows toward the cooler side (furnace door) during this step until solidification of the flux near 890°C. Once the proper position in the furnace is located, the self-decanting process is reproducible, as shown in Figure 2; however, replacement of heating elements generally requires re-determination of the optimum position. With the proper temperature gradient, abundant harvests of $YBa_2Cu_3O_x$ platelets up to several tenths of a millimeter in thickness and averaging 1-3 mm in width, as shown in Figure 3, have been consistently obtained. The platelets grow parallel to one another and perpendicular to the crucible bottom; they tend to be affixed

---

1. 980°C for Gd,Dy,Ho; 990°C for Y,Pr,Er,Tm,Yb; 1005°C for Nd,Sm,Eu. Except for Y, these soak temperatures represent successful but not optimized conditions.

2. In some experiments, samples were cooled at this rate to 450°C and held for up to several weeks in air. This procedure did not, however, reliably result in optimum transition temperatures and widths. Most frequently, improvement was obtained by a post-growth oxygen anneal.

by their corners and large pieces are easily recovered by gently rocking against the platelet with the shaft of a needle placed between the crystals. Smaller crystals are readily dislodged with the needle tip. Crystal orientation was found to be very sensitive to the gradient. In cases where a near-complete decant was achieved but the platelets were oriented parallel to the crucible bottom, and thus impossible to extract, moving the crucible 1-2 cm toward the cooler side (furnace door) resulted in complete self-decantation and the desired platelet orientation. Harvested crystals were annealed under 1 atm flowing oxygen using several different heating programs.

To grow $Nd_{1.85}Ce_{0.15}CuO_4$ crystals, a charge composition stoichiometric in the Nd/Ce ratio with a 6-7-fold molar excess of CuO was chosen. This composition has been shown in other work [40,41] to yield crystals with the desired level of Ce-substitution. Nd_2O_3, "active" CeO_2 (prepared by decomposing cerium carbonate at 650°C in air overnight), and CuO of 99.99% or higher purity were mixed in a Nd:Ce:Cu mol ratio of 1.85:0.15:8 by grinding 30 min. In a typical run, approximately 10 g charge was packed into a 5-ml high-form alumina crucible. The charge crucible was supported in a larger porcelain crucible approximately half-filled with alumina powder. A vertical temperature gradient was achieved by pushing the charge crucible several mm down into the alumina powder. The double-crucible was centered

in a 1200°C muffle furnace[3] (Lindberg Model 51442) and heated in air: 1) from ambient to 1200°C in 4 h, soak 2 h; 2) step-cool in 5 min to 1150°C, stabilize 30 min; 3) cool at 4°/h to 950°C; 4) cool in 12 h to ambient. The self-decant was radially symmetric, leaving numerous shiny platelets with faces parallel to the crucible bottom; small pieces could be mechanically extracted. Superconductivity was induced by heating crystals under flowing argon (99.998%, 1 atm) in 2 h to 900°C, soaking 14 h, and cooling in 2 h to ambient.

SAMPLE CHARACTERIZATION

$YBa_2Cu_3O_x$ crystals were checked for impurities by energy-dispersive X-ray spectroscopy (EDX) using a scanning electron microscope (Amray 1400, Tracor TN2000 analyzer). Clean crystal surfaces were impurity-free within the limits of this method; however, trace levels of zirconium were just detectable in frozen flux droplets on crystal faces. Analyses of the $Nd_{1.85}Ce_{0.15}CuO_4$ crystals were consistent with the desired level of Ce-substitution; the use of alumina containers, as has been reported by others [41], did not lead to detectable Al incorporation. This is likely attributable to the relatively short heating times and absence of BaO in the flux.

---

3. Although temperature gradients are readily established in tube-type furnaces, a number of experiments in both the Nd-Ce-Cu-O and Y-Ba-Cu-O systems resulted in good decantation but little or no crystal growth. The best results were obtained using muffle-type furnaces.

Superconducting transitions were determined by single-crystal AC susceptibility measurements. A single-coil, self-inductance system similar to that used for measuring thin films [42] and a double-coil mutual inductance configuration (which allowed measurements of the out-of-phase component of the susceptibility) were used. A typical coil consisted of approximately 100 turns of 25-μm wire with a 1 mm inner diameter and 3 mm outer diameter. Most measurements were conducted at 10 kHz with a current of 150 μA which generated fields of less than 100 mOe and permitted detection of shielding from sub-millimeter-sized crystals. The coil was situated on a copper block at the end of a cryostat-insert. A crystal was centered in or on the coil (depending on its size), a diode thermometer was placed on top of the sample, and the entire block-coil-sample-thermometer structure was wrapped with teflon tape that served as insulation. The probe was then capped with a perforated copper can and slowly immersed into a helium dewar. This procedure permitted fast sample screening with absolute temperature errors of less than 1 K and without exposing crystals to grease or glue.

Single-crystal resistivity data were obtained using a standard four-probe DC technique. The sample was mounted on a magnesium oxide substrate and four 25-μm gold wires were attached in an in-line geometry using silver paint. The silver paint was "fixed" to the crystal by heating in air for 30 min at approximately 350°C. The substrate was then attached with grease to a copper cold finger containing a heater and a carbon-glass thermometer. Resistivity was measured while cooling the sample in a

helium gas-flow cryostat. Within several degrees of and during the superconducting transition, the sample was slowly cooled at approximately 100 mK/min; in other temperature regions, at approximately 500 mK/min.

The c-axes of individual crystal pieces were measured by X-ray diffraction using 1) a single-crystal diffractometer and 2) a powder diffractometer. Both methods were used for value-comparison purposes, as X-ray diffraction represents the only reasonable method for routinely estimating the oxygen content of individual crystals. In method 1, each crystal was mounted and aligned on an automated Picker four-circle diffractometer. Step scans in $\pm 2\theta$ were taken of the (0,0,11) and (0,0,$\bar{1}1$) peaks in 0.02° steps. The diffraction profiles were then least-squares fitted to double-Gaussian curves to determine the positions of the Cu $K\alpha_1$ and $K\alpha_2$ peaks from which the value of the c-axis was calculated. In method 2, the (00ℓ) reflections of individual crystal-pieces were scanned using Cu $K\alpha$ radiation and a Scintag PAD V (2θ:θ) powder diffractometer, radius 220 mm, with a receiving-slit acceptance angle of 0.07° and a step-size of 0.01°. Individual crystals were mounted with a flat platelet-face parallel to the surface of an off-axis-cut single-crystal quartz substrate and held in place with a thin film of petroleum jelly. A manual omega (θ) scan about the position for the (006) reflection was used to define the (horizontal) position of the diffraction vector relative to the omega (θ) axis. 2θ:θ scans of the (00ℓ) reflections were then recorded with the θ-angle offset by this constant amount. No adjustment for possible (vertical) tilt was attempted. The

resultant c-axis parameters were calculated by least-squares refinement [43] of the α_1 2θ-values for the (00ℓ) reflections. Literature data [44] on the correlation of c-axis length vs. oxygen content, obtained from iodometric and X-ray diffraction analyses of bulk ceramic samples, were used to derive the linear relationship

$$x = 74.49 - 5.787c \ , \qquad \text{(Eqn. 1)}$$

where c is the c-axis cell parameter in Å and x is the oxygen content in $YBa_2Cu_3O_x$.[4] Using this relationship for individual crystals, the estimated uncertainty in oxygen content is ±0.04 mol; the random and systematic errors inherent in determining the c-axis by X-ray diffraction are minor compared to the scatter in the data used to derive Eqn. 1.

RESULTS AND DISCUSSION

$YBa_2Cu_3O_x$ System

In addition to developing a reproducible protocol for the growth of large crystals one to several millimeters on an edge, a post-growth oxygen-annealing study was conducted with the aim of identifying the optimum conditions to reproducibly yield maximum T_c values and minimum transition widths. The results of this

---

4. The data-pairs used to derive Eqn. 1 include values for 1) tetragonal $YBa_2Cu_3O_{6.0}$ from a single-crystal structure determination [45], and 2) a near-fully oxygenated, high-quality (purity and T_c) polycrystalline sample that was synthesized and analyzed by bromo/iodometric titration [46] in our own laboratory (a = 3.8838(8), b = 3.8164(4), c = 11.664(1) Å; x = 6.98±0.01).

study were variable. Typically, as shown in Figure 4, oxygen-annealing tended to sharpen transitions and raise T_c. Exceptions were noted, however, and occasionally well-oxygenated crystals resulted from the slow-cooling step in air at the end of the crystal growth program, as illustrated in Figure 5. "Crystal quality", as defined by T_c values and transition widths determined by AC susceptibility measurements, was often observed to vary within a single growth- and oxygen-anneal-batch. For other batches, the scatter in T_c values and transition widths was minimal and on the order of tenths of a degree. Accounting for these variations is difficult, as synthetic conditions were kept as uniform as possible (container material, reagent lots, etc.) and significant differences in "batch morphology" (especially crystal thicknesses) were not observed. The data shown in Figure 6 are representative of the "better" crystal-batches; according to the susceptibility curve, a T_c onset near 92 K is indicated with a transition width of 0.5 K.

In an effort to determine an optimum post-growth oxygen annealing program, several different heating profiles, given in Figure 7, were studied. A correlation was sought with T_c and transition width (from single-crystal AC susceptibility curves) and oxygen content (estimated from the c-axis cell parameter). The results are collected in Table 1, in which the entries are ordered in decreasing c-axis or increasing apparent oxygen content. The following observations were made.

1) As can be seen by comparing oxygen contents with T_c values in Table 1, for x-values in $YBa_2Cu_3O_x$ near and above 6.8,

T_c is relatively insensitive. This observation is consistent with detailed neutron-diffraction structural studies of chemically analyzed ceramic samples [47,48]; i.e., although the unit cell c-axis parameter is sensitive to oxygen-content in the x = 6.8-7.0 region, a near-plateau in T_c vs. oxygen content occurs in this x-range. With decreasing oxygen content, near x = 6.7-6.8, a significant decline in T_c commences, as can be seen by comparing crystals 1 and 2 in Table 1.

2) The "best" crystals; i.e. maximum T_c and minimum transition width by AC susceptibility, were not those with minimum c-axis lengths and thus maximum "apparent" oxygen content (see crystals 21-25 in Table 1). In the T_c vs. oxygen plateau region (x = 6.8-7.0), microstructural and/or microchemical factors other than overall oxygen content and/or oxygen-ordering may be important in determining the details of the transition.

3) For a single oxygen annealing program, longer hold times during the final soak below red heat did not consistently improve properties (compare crystals 5 with 11, and 12 with 14 in Table 1).

4) The "best" crystals (entries 4, 5, 8, 9, 14, and 15 in Table 1) exhibiting the highest T_c values and minimum transition widths were obtained from a number of different growth-batches and were oxygen-annealed with substantially different heating profiles. Final soak temperatures ranged from 470 to 565°C, times from 72 to 504 h. The "apparent" oxygen content as indicated by the c-axis lengths ranged from 6.80 to 6.86 mol.

5) The definition of "crystal quality" has a subjective component that depends on measurement technique. Figure 8 shows the in- and out-of-phase components of the AC susceptibility of what might be considered a "good" crystal that exhibits a sharp transition with a width of 0.7 K. Yet, as the multiple peaks of the out-of-phase trace demonstrate, an additional anomalous loss occurs during the apparently sharp transition. These loss-peaks could be attributable to granular effects, or domains of superconducting phases with slightly different transition temperatures.

6) Despite the often variable results observed for different post-growth oxygen-annealing protocols, the following heating profile is suggested as a reasonable starting point for the preparation of $YBa_2Cu_3O_x$ crystals with maximum T_c values and minimum transition widths:

1. Heat at 50-100°/h to 800-850°C.
2. Cool at 1-3°/h to 750°C; soak 4 d.
3. Cool in 48 h to 500°C; soak 5 d.
4. Cool in 24 h to ambient.

Crystals should be slow-cooled from growth temperatures (10-20°/h) rather than quenched.

$RBa_2Cu_3O_7$

AC susceptibility curves for crystals of the Dy and Ho analogs of $YBa_2Cu_3O_x$ are shown in Figure 9. For $DyBa_2Cu_3O_x$, T_c occurs near 92.2 K with a transition width of 1 K; for

$HoBa_2Cu_3O_x$, 91.7 K with a width of 1 K. Both crystals were annealed with program V (Figure 7). Figure 10 shows AC susceptibility curves for nine $RBa_2Cu_3O_x$ crystals; R = Ho, Yb, Gd, Dy, Tm, Er, Eu, Sm, and Nd. The Pr congener was not superconducting, although well-formed crystals were readily obtained. As can be seen in Figure 10, many of the transitions are relatively broad, especially that of $NdBa_2Cu_3O_x$. All crystals had been oxygen-annealed, but no attempt was made to optimize either the growth or annealing conditions. The growth-mixture melt temperatures were observed to vary considerably for the different rare earths, thus each system requires individual optimization.

$Nd_{1.85}Ce_{0.15}CuO_4$

Measurements of the c-axis unit cell parameters of several crystals indicated lengths of 12.057 Å, as compared to 12.153(1) Å for Nd_2CuO_4. This is consistent with the target level of Ce-substitution [8] and elemental analyses by SEM/EDX. AC susceptibility curves for very small platelet-fragments of as-grown and Ar-annealed samples are shown in Figure 11, and indicate a T_c onset near 24 K for the Ar-annealed fragment. Work is continuing to optimize growth conditions for this system so that larger superconducting crystals can be routinely obtained.

CONCLUSIONS

The self-decanting flux technique is a reliable procedure for the growth of nearly-free-standing crystals of the $YBa_2Cu_3O_7$-type phases. Preliminary experiments were successful in modify-

ing the method to grow $Nd_{1.85}Ce_{0.15}CuO_4$ crystals, indicating that this approach may have general applicability for all of the superconducting cuprates that can be prepared from non-volatile reactants. Oxygen-annealing studies of $YBa_2Cu_3O_x$ crystals have shown that samples obtained from any single annealing procedure following carefully controlled crystal growth conditions may or may not exhibit optimized superconducting properties. A single "optimal" annealing procedure may not exist. Indeed, previous studies [6,11,16,19-21,24,29,49] report widely varying annealing profiles in both air and pure oxygen that can result in $YBa_2Cu_3O_x$ crystals with sharp transitions near 92 K. In addition to time, temperature, and atmosphere, oxidation kinetics may be dependent upon microstructural and/or microchemical variations from crystal to crystal, even within a single growth batch. Furthermore, although optimal superconducting properties in the $YBa_2Cu_3O_7$ system without question require well-oxygenated samples, the influence of cation-site defects/disorder is both unclear and difficult to assess experimentally [50]. Each crystal may be considered at the microscopic level as having a kinetically unique sample history; unfortunately, the detailed superconducting properties are apparently sensitive to this level of sample variability.

Knowledge and control of the detailed structure-property relations in $YBa_2Cu_3O_x$ will require reliable probes of microchemical and microstructural variation. Recently, Raman studies of the Cu-O vibrational frequencies in single crystals were reported [49] as being sensitive to sample homogeneity and optimized

superconductivity. In addition, high-resolution X-ray studies of $YBa_2Cu_3O_x$ crystals using a synchrotron source [51] have indicated "subgrains" with slightly differing orthorhombicity that indicate a multiphase character, and which might be linked to granular superconductivity.

ACKNOWLEDGMENTS

We thank R. Woolever for the SEM/EDX analyses and D. Cornelius for photography. The crystal growth method would not have been developed without seminal suggestions from L.F. Schneemeyer. This work was funded by the Office of Naval Research.

REFERENCES

[1] L.F. Schneemeyer, in: Chemistry of Superconductor Materials, Ed. T.A. Vanderah (Noyes, NJ, 1991).

[2] Crystal Growth 1989, Proceedings of the Ninth International Conference on Crystal Growth (Sendai, Japan, 22-25 August 1989), Eds. J. Chikawa, J.B. Mullin, and J. Woods., Eds., J. Crystal Growth 99 (1990) 915-975.

[3] High-Tc Superconductors: Materials Aspects II, Eds. D. Elwell, M. Schieber, and L. Schneemeyer, Special Issue, J. Crystal Growth 91 (1988) 249-469.

[4] High-Tc Superconductors: Materials Aspects, Eds. D. Elwell, M. Schieber, and L. Schneemeyer, Special Issue, J. Crystal Growth 85 (1987) 563-665.

[5] R.A. Laudise, L.F. Schneemeyer, and R.L. Barns, J. Crystal Growth 85 (1987) 569.

[6] H.J. Scheel, J. Less-Common Metals 151 (1989) 199.

[7] Y. Tokura, H. Takagi, and S. Uchida, Nature 337 (1989) 345.

[8] H. Takagi, S. Uchida, and Y. Tokura, Phys. Rev. Lett. 62 (1989) 1197.

[9] A.C.W.P. James and D.W. Murphy, in: Chemistry of Superconductor Materials, Ed. T.A. Vanderah (Noyes, NJ, 1991).

[10] L.F. Schneemeyer, J.V. Waszczak, T. Siegrist, R.B. van Dover, L.W. Rupp, B. Batlogg, R.J. Cava, and D.W. Murphy, Nature 32 (1987) 601.

[11] D.L. Kaiser, F. Holtzberg, M.F. Chisholm, and T.K. Worthington, J. Crystal Growth 85 (1987) 593.

[12] Y. Hidaka, Y. Enomoto, M. Suzuki, M. Oda, and T. Murakami, J. Crystal Growth 85 (1987) 581.

[13] G. Balestrino, S. Barbanera, and P. Paroli, J. Crystal Growth 85 (1987) 585.

[14] R.A. Laudise, L.F. Schneemeyer, and R.L. Barns, J. Crystal Growth 85 (1987) 569.

[15] H. Katayama-Yoshida, Y. Okabe, T. Takahashi, T. Sasaki, T. Hirooka, T. Suzuki, T. Ciszek, and S.K. Deb, Japan. J. Appl. Physics 26(12) (1987) L2007.

[16] G. Balestrino, S. Barbanera, G. Castellano, V. Foglietti, M. Giammatteo, Y.L. Liu, P. Paroli, and F. Scarinci, Mater. Res. Bull. 23 (1989) 1119.

[17] T. Konaka, I. Sankawa, and M. Sato, J. Crystal Growth 91 (1988) 278.

[18] J. Wojcik, M. Rosochowska, H. Niculescu, and A. Pajaczkowska, J. Crystal Growth 91 (1988) 255.

[19] C.N.W. Darlingtion, D.A. O'Connor, and C.A. Hollin, J. Crystal Growth 91 (1988) 308.

[20] W. Sadowski and H.J. Scheel, J. Less-Common Metals 150 (1989) 219.

[21] M.J.V. Menken, K. Kadowaki, and A.A. Menovsky, J. Crystal Growth 96 (1989) 1002.

[22] W. Qianzhang, X. Xiaozhen, C. Yingchuan, J. Peizhi, D. Hongmin, H. Jiashan, C. Bingyu, H. Xueli, L. Yanyan, and T. Disheng, Mater. Res. Bull. 24 (1989) 1325.

[23] R. Boutellier, B.N. Sun, H.J. Scheel, and H. Schmid, J. Crystal Growth 96 (1989) 465.

[24] F. Holtzberg and C. Feild, J. Crystal Growth 99 (1990) 915.

[25] K. Oka and H. Unoki, J. Crystal Growth 99 (1990) 922.

[26] S. Bosi, T. Puzzer, G.J. Russell, S.L. Town, and K.N.R. Taylor, J. Mater. Sci. Lett. 8 (1989) 497.

[27] S.L. Town, B.A. Hunter, S. Bosi, R.L. Davis, and K.N.R. Taylor, Physica C 165 (1990) 298.

[28] P. Murugaraj, J. Maier, and A. Rabenau, Solid State Commun. 71 (1989) 167.

[29] D.L. Kaiser, F. Holtzberg, B.A. Scott, and T.R. McGuire, Appl. Phys. Lett. 51 (1987) 1040.

[30] W. Zhang, K. Osamura, and S. Ochiai, J. Am. Ceram. Soc. 73 (1990) 1958.

[31] R.S. Roth, J.R. Dennis, and K.L. Davis, Adv. Ceramic Mat. 2 (1987) 303.

[32] B.-J. Lee and D.N. Lee, J. Am. Ceram. Soc. 74 (1991) 78.

[33] D.L. Kaiser, F.W. Gayle, R.S. Roth, and L.J. Swartzendruber, J. Mater. Res. 4 (1989) 745.

[34] J. Giapintzakis, D.M. Ginsberg, and P.-D. Han, J. Low-Temp. Phys. 77 (1989) 155.

[35] H. Schmid, E. Burkhardt, N.B. Sun, and J.-P. Rivera, Physica C 157 (1989) 555.

[36] T. Hatanaka and A. Sawada, Japan. J. Appl. Phys. 28 (1989) L794.

[37] A. Drake, J.S. Abell, and S.D. Sutton, J. Less-Common Met. 164/165 (1990) 187.

[38] Y. Wang, L.W.M. Schreurs, P. Van der Linden, Y. Li, and P. Bennema, J. Crystal Growth 106 (1990) 487.

[39] T. Wolf, W. Goldacker, B. Obst, G. Roth, and R. Fluekiger, J. Crystal Growth 96 (1989) 1010.

[40] Y. Dalichaouch, B.W. Lee, C.L. Seaman, J.T. Markert, and M.B. Maple, Phys. Rev. Lett. 64 (1990) 599.

[41] W. Sadowski, M. Affronte, M. Francois, E. Koller, and E. Walker, J. Less-Common Met. 164/165 (1990) 824.

[42] J.H. Classen, M.E. Reeves, and R.J Soulen, Jr., Rev. Sci. Instr. 62 (1991) 996.

[43] Locally-modified version of PODEX; C. Foris, Powder Diffraction 1 (1986) 66.

[44] M.E. Parks, A. Navrotsky, K. Mocala, E. Takayama-Muromachi, A. Jacobson, and P.K. Davies, J. Solid State Chem. 79 (1989) 53.

[45] J.S. Swinnea and H. Steinfink, J. Mater. Res. 2(4) (1987) 425.

[46] E.H. Appelman, L.R. Morss, A.M. Kini, U. Geiser, A. Umezawa, G.W. Crabtree, and K.D. Carlson, Inorg. Chem. 26(20) (1987) 3237.

[47] R.J. Cava, A.W. Hewat, E.A. Hewat, B. Batlogg, M. Marezio, K.M. Rabe, J.J. Krajewski, W.F. Peck Jr., and L.W. Rupp, Physica C 165 (1990) 419.

[48] J.D. Jorgensen, B.W. Veal, A.P. Paulikas, L.J. Nowicki, G.W. Crabtree, H. Claus, and W.K. Kwok, Phys. Rev. B 41 (1990) 1863.

[49] L. Nganga, P.V. Huong, J.P. Chaminade, P. Dordor, K. Froehlich, and M. Jergel, J. Less-Common Met. 164/165 (1990) 208.

[50] M. Tinkham and C.J. Lobb, in: Solid State Physics, Advances in Research and Applications, Eds. H. Ehrenreich and D. Turnbull (Academic Press, NY, 1989) pp. 91-134.

[51] H.You, J.D. Axe, X.B. Kan, S.C. Moss, J.Z. Liu, and D.J. Lam, Phys. Rev. B 37 (1988) 2301.

FIGURE CAPTIONS

Fig. 1 Temperature data about the crucible during the high-temperature soak in a typical $YBa_2Cu_3O_x$ crystal growth experiment.

Fig. 2 Crucibles from a series of $YBa_2Cu_3O_x$ crystal growth experiments illustrating reproducible "self-decant fans" once the temperature differences shown in Fig. 1 are established.

Fig. 3 $YBa_2Cu_3O_x$ crystals obtained with the self-decanting method. (1 division = 1 mm)

Fig. 4 Normalized AC susceptibility curves for an unannealed and oxygen-annealed $YBa_2Cu_3O_x$ crystal from the same growth-batch indicating the typical improvement in superconducting properties.

Fig. 5 AC susceptibility curve (arbitrary units) for a $YBa_2Cu_3O_x$ crystal that was slow-cooled in air from growth temperatures but not oxygen-annealed; unusually good superconducting properties are observed.

Fig. 6 Single-crystal resistivity and AC susceptibility (arbitrary units) curves for a representative "high-quality" $YBa_2Cu_3O_x$ crystal. The crystal was annealed under oxygen at 565°C for 4 d; similar results were obtained for crystals annealed for 7 d at the same temperature.

Fig. 7 Various oxygen-annealing programs for the $YBa_2Cu_3O_x$ crystals listed in Table 1. Crystals were heated under flowing oxygen at 1 atm.

Fig. 8 In- and out-of-phase components of the AC susceptibility curve for an oxygen-annealed $YBa_2Cu_3O_x$ crystal. Although this might be considered a "good" crystal with a sharp transition approximately 0.7 K wide, the out-of-phase trace indicates an additional anomalous loss during the apparently sharp transition.

Fig. 9 Normalized AC susceptibility curves for an oxygen-annealed $HoBa_2Cu_3O_x$ and $DyBa_2Cu_3O_x$ crystal. These transitions represent the best results obtained in preliminary experiments extending the self-decanting growth method to the $RBa_2Cu_3O_x$ series.

Fig. 10 Normalized AC susceptibility curves for nine oxygen-annealed $RBa_2Cu_3O_x$ crystals illustrating the general results obtained in preliminary crystal growth experiments; the $PrBa_2Cu_3O_x$ crystals were not superconducting and the $NdBa_2Cu_3O_x$ crystals typically displayed very broad transitions. The details of the growth procedure need to be optimized for each $RBa_2Cu_3O_x$ system.

Fig. 11 AC susceptibility curves (arbitrary units) for small as-grown and argon-annealed $Nd_{1.85}Ce_{0.15}CuO_4$ platelet-fragments from the same growth-batch, indicating the development of superconductivity above 20 K in the annealed sample.

TABLE 1 Results of Oxygen-Annealing Studies of Individual $YBa_2Cu_3O_x$ Crystals

Crystal	Growth Batch	c-axis[1], Å	c-axis[2], Å	O-content, mol x	Transition, K 90%[3]	10%	ΔT_c, K	Annealing Program[4]
1	B	11.719		6.67	78.8	60.3	18.5	unannealed
2	J		11.703	6.76	93.9	90.9	3.0	unannealed
3	J		11.698	6.79	93.2	91.3	1.9	i
4	A		11.696	6.80	92.4	92.0	0.4	ii; t = 336 h
5	B	11.696	11.695	6.80/6.81	92.9	92.6	0.3	iii; t = 72 h
6	A	11.694		6.81	92.5	90.8	1.7	ii; t = 336 h
7	A	11.692		6.82	93.1	89.6	3.5	ii; t = 336 h
8	A	11.691	11.695	6.83/6.81	92.5	92.1	0.4	ii; t = 504 h
9	C		11.692	6.82	93.0	92.4	0.6	i
10	C	11.691		6.83	93.8	93.0	0.8	i
11	B	11.689	11.693	6.84/6.82	92.2	88.2	4.0	iii; t = 144 h
12	A	11.689	11.691	6.84/6.83	92.4	91.0	1.4	ii; t = 672 h
13	A	11.689		6.84	93.1	92.4	0.7	ii; t = 336 h
14	A	11.688	11.691	6.85/6.83	92.6	92.1	0.5	ii; t = 504 h
15	C		11.687	6.85	93.0	92.8	0.2	iv; t = 488 h
16	H		11.686	6.86	91.9	91.5	0.4*	v
17	J		11.685	6.86	91.8	90.9	0.9	iv; t = 372 h
18	G	11.685		6.86	92.4	90.9	1.5	v
19	A	11.684		6.87	92.7	90.8	1.9	ii; t = 168
20	I		11.684	6.87	94.2	93.1	1.1	iv; t = 200 h
21	K		11.683	6.88	94.0	91.9	2.1	v
22	E	11.683		6.88	92.1	90.4	1.7	v
23	F	11.680		6.89	92.6	90.6	2.0	v
24	H	11.679		6.90	91.5	90.7	0.8	v
25	D	11.675		6.92	92.7	88.3	4.4*	v

[1]determined using powder diffractometer
[2]determined using single-crystal diffractometer
[3]percentages indicate fraction of total change in AC susceptibility
[4]annealing programs are given in Figure 7
*entries marked with an asterisk exhibited transitions with features and/or long tailing to reach saturation

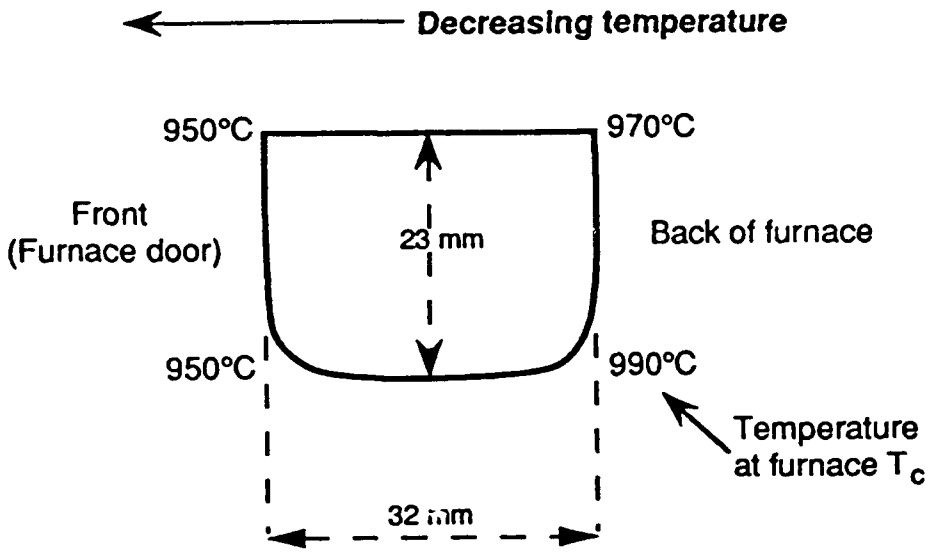
Decreasing temperature
950°C
970°C
Front
(Furnace door)
23 mm
Back of furnace
950°C
990°C
Temperature
at furnace T_c
32 mm

Figure 1

Fig 2

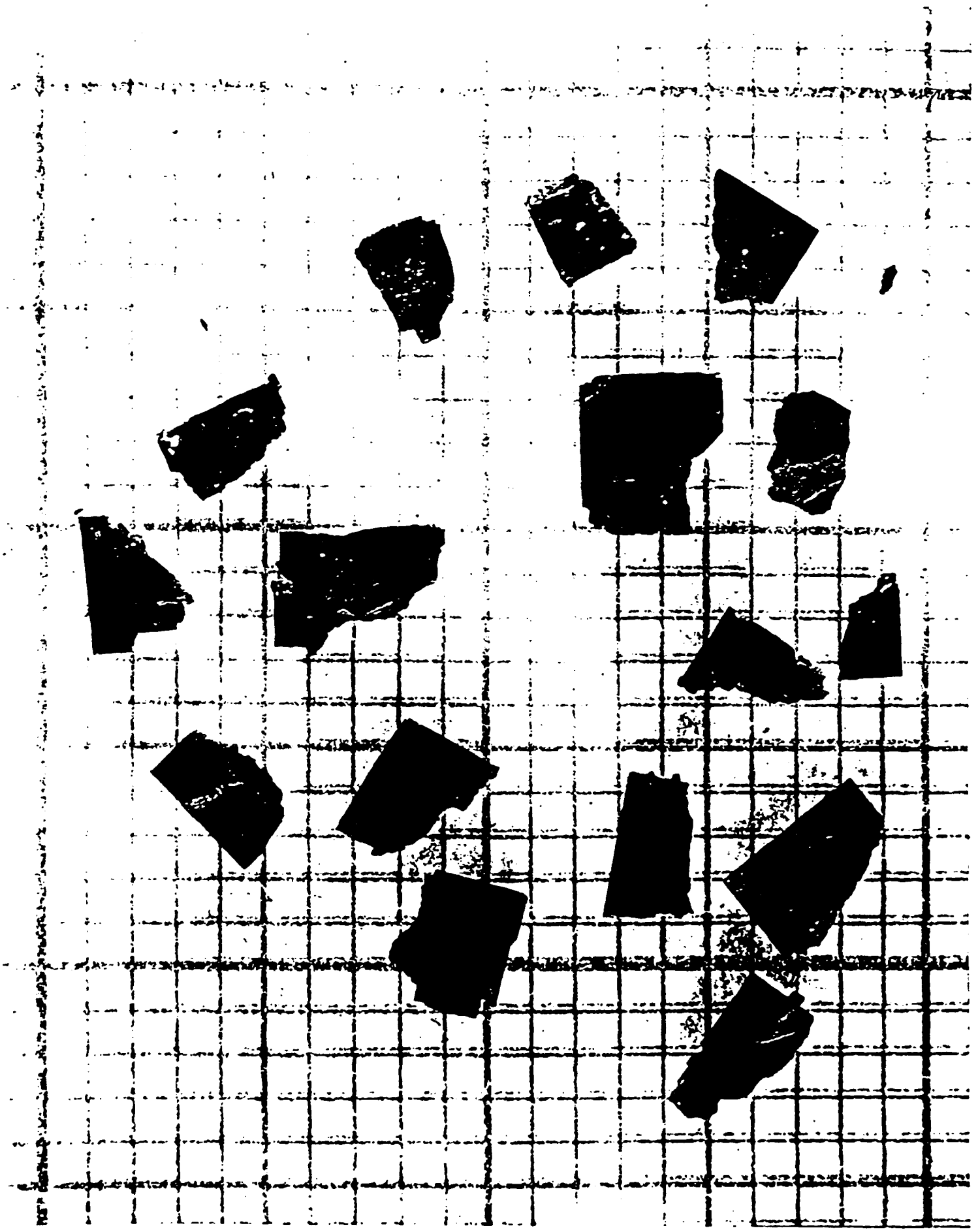

Fig 3

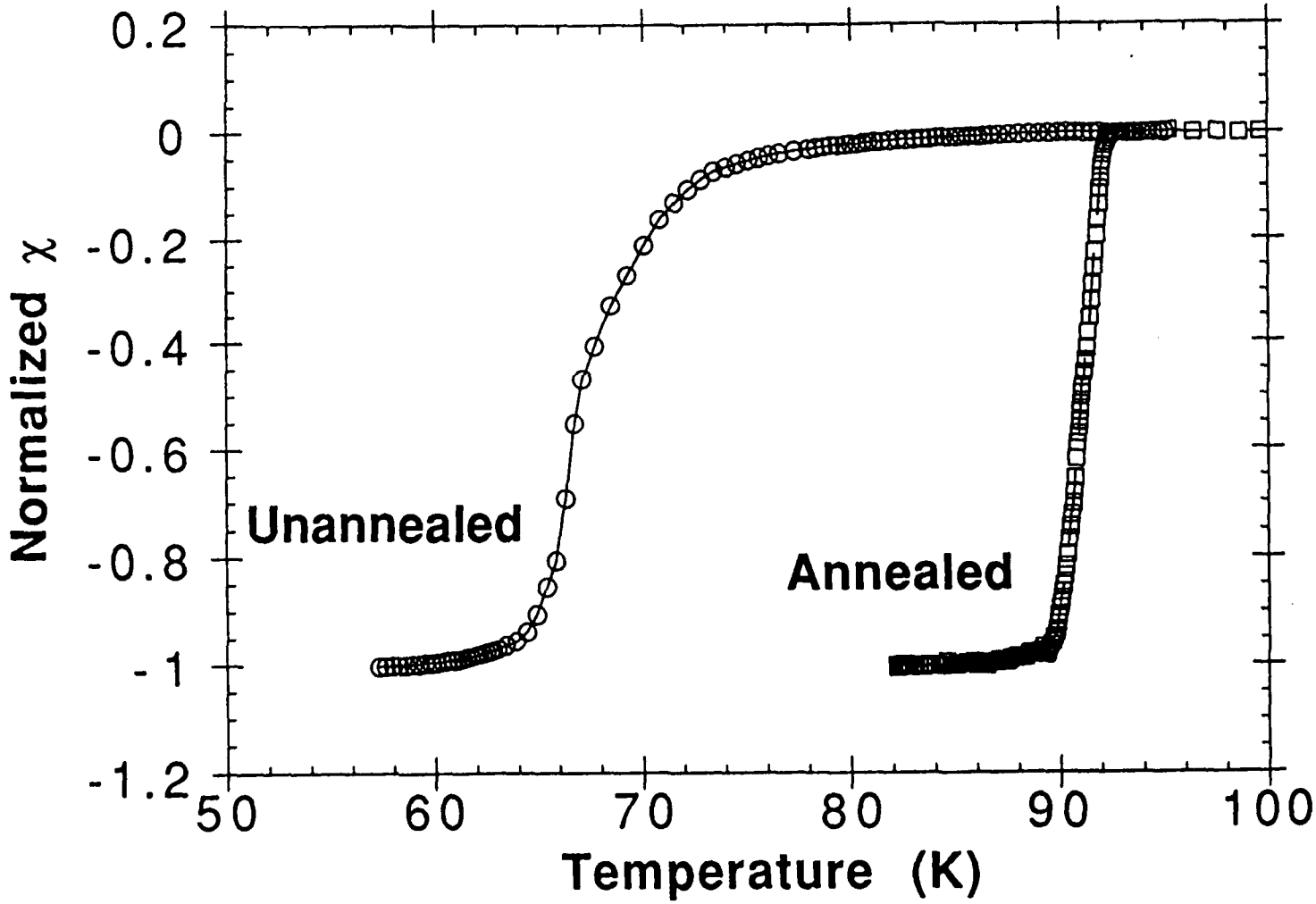
0.2
0
-0.2
-0.4
-0.6
-0.8
-1
-1.2
Normalized χ
Unannealed
Annealed
50
60
70
80
90
100
Temperature (K)

Figure 4

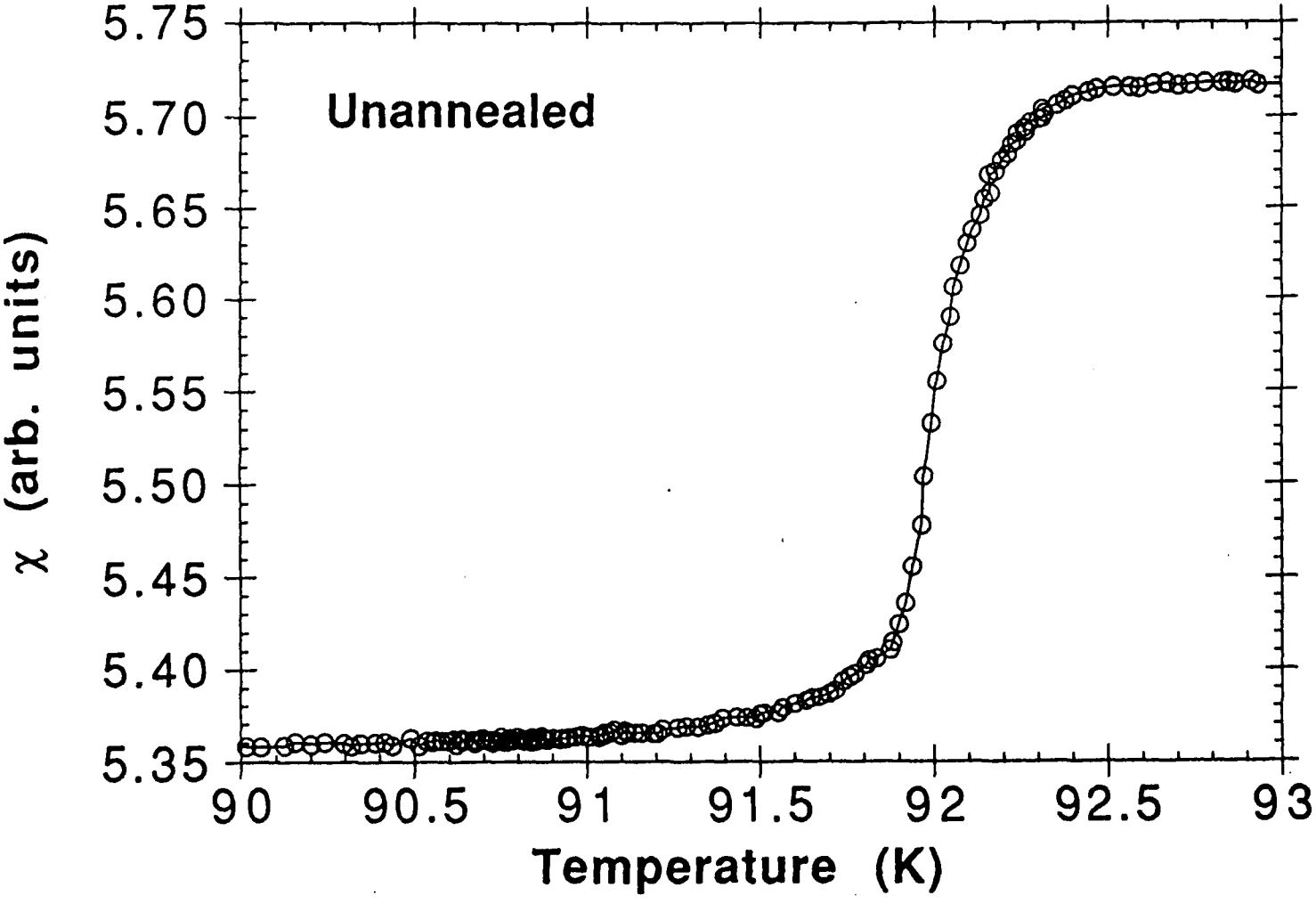
Unannealed
χ (arb. units)
5.75
5.70
5.65
5.60
5.55
5.50
5.45
5.40
5.35
90
90.5
91
91.5
92
92.5
93
Temperature (K)

Figure 5

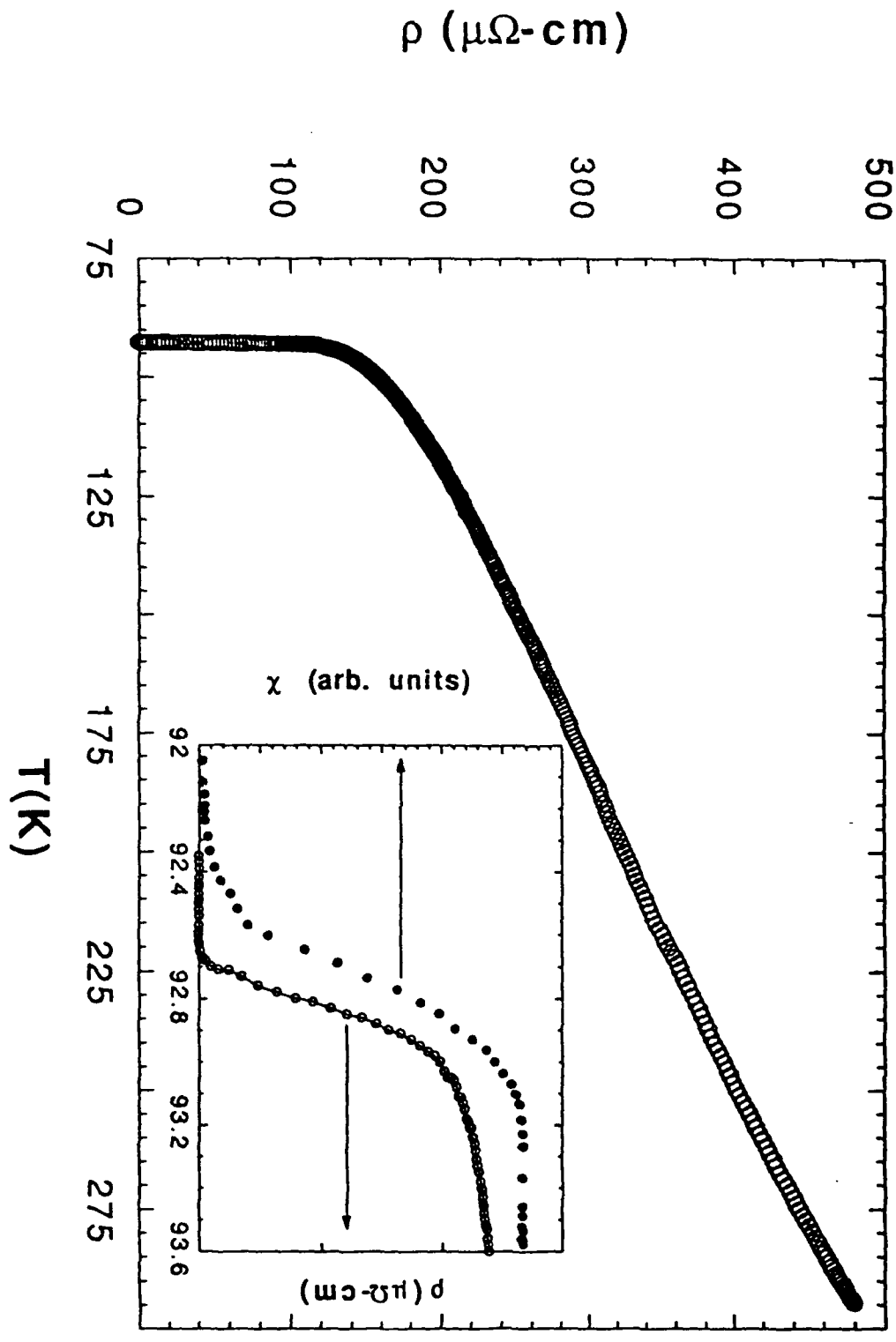
ρ (μΩ-cm)
0
100
200
300
400
500
T(K)
75
125
175
225
275
χ (arb. units)
92
92.4
92.8
93.2
93.6
ρ (μΩ-cm)

Figure 6

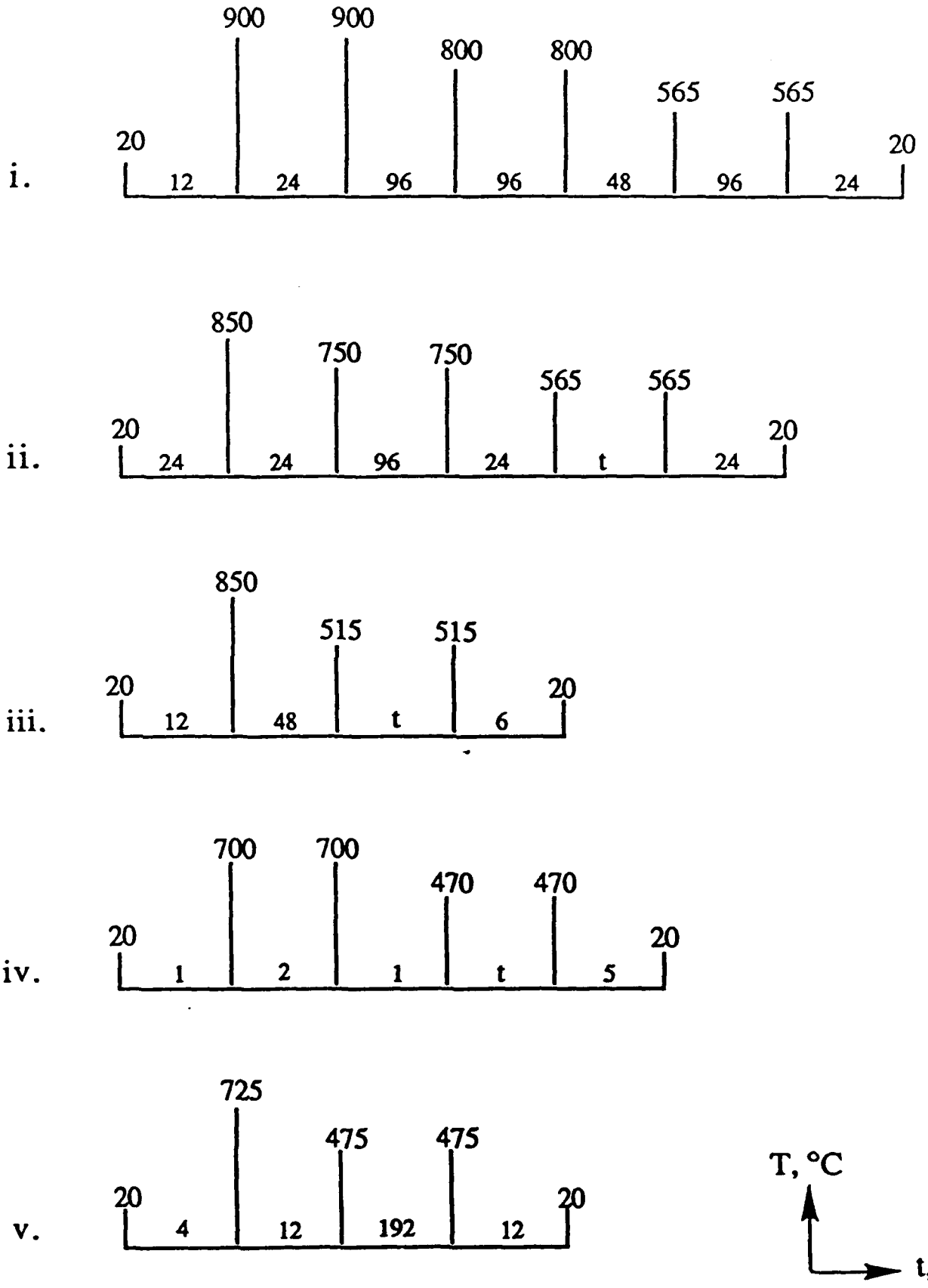
i.
20
900
900
800
800
565
565
20
12
24
96
96
48
96
24
ii.
20
850
750
750
565
565
20
24
24
96
24
t
24
iii.
20
850
515
515
20
12
48
t
6
iv.
20
700
700
470
470
20
1
2
1
t
5
v.
20
725
475
475
20
4
12
192
12
T, °C
t, h

Figure 7

Figure 8

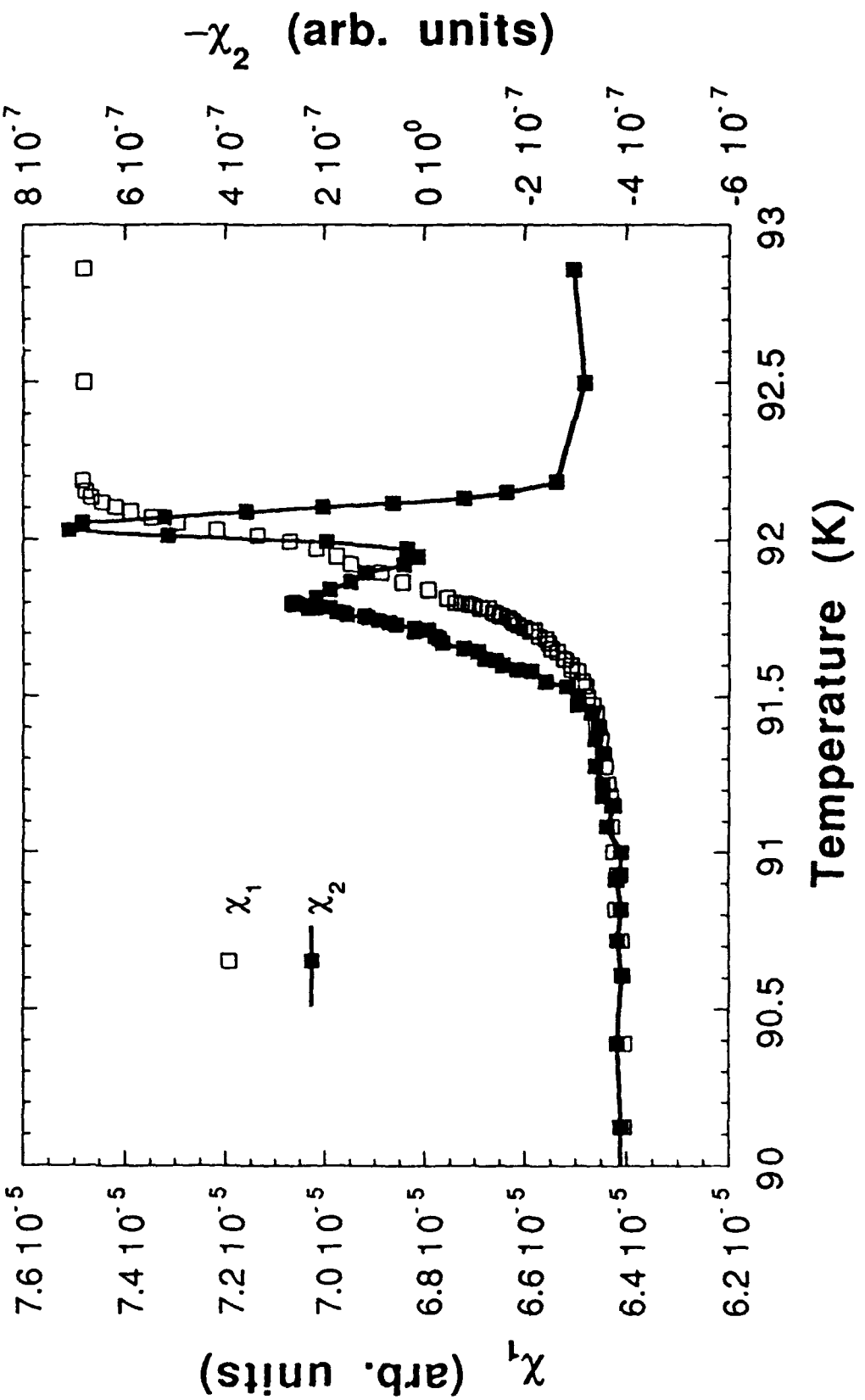
$-\chi_2$ (arb. units)
8 10^{-7}
6 10^{-7}
4 10^{-7}
2 10^{-7}
0 10^{0}
-2 10^{-7}
-4 10^{-7}
-6 10^{-7}
93
92.5
92
91.5
91
90.5
90
Temperature (K)
χ_1
χ_2
χ_1 (arb. units)
7.6 10^{-5}
7.4 10^{-5}
7.2 10^{-5}
7.0 10^{-5}
6.8 10^{-5}
6.6 10^{-5}
6.4 10^{-5}
6.2 10^{-5}

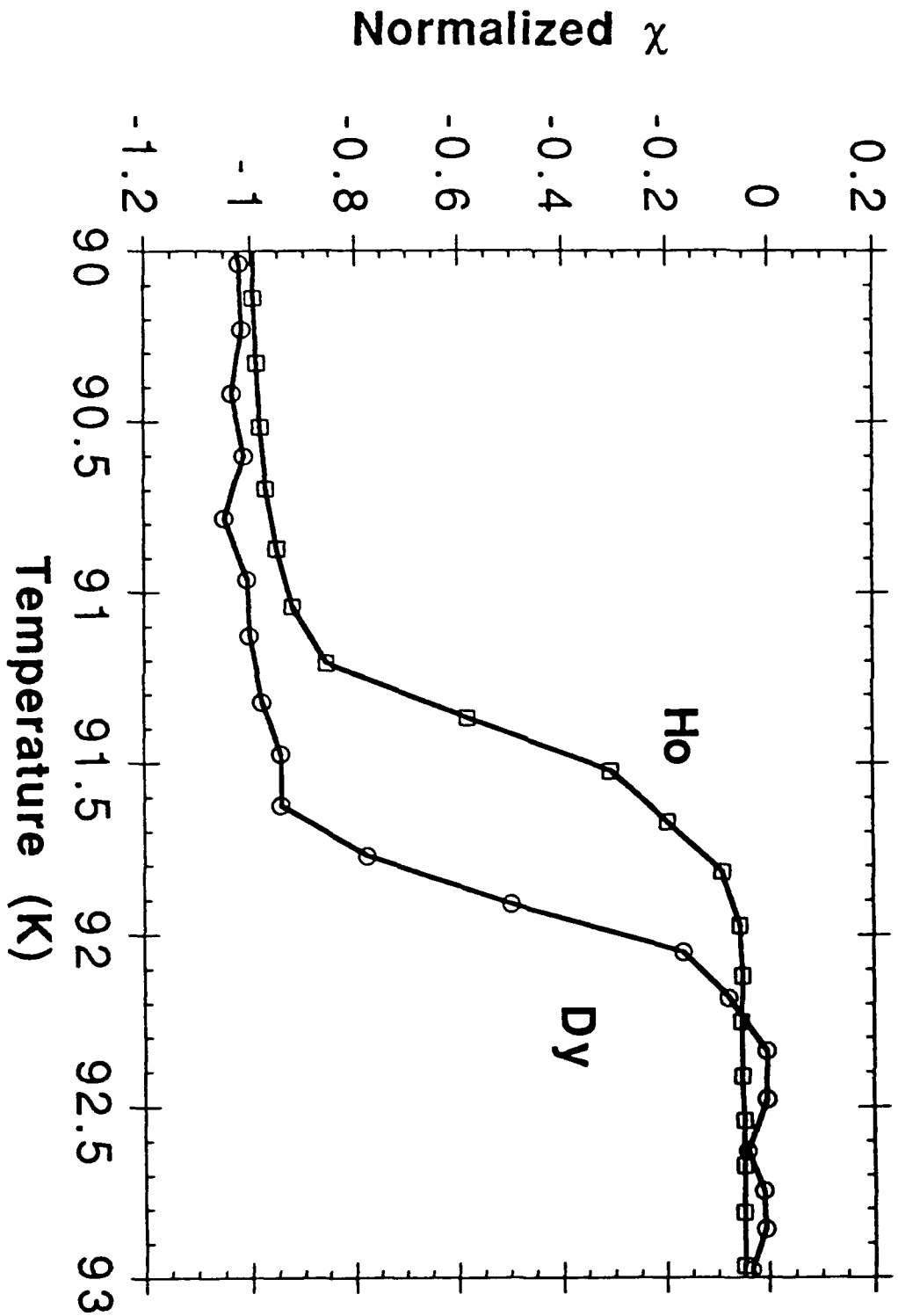
Normalized χ
-1.2
-1
-0.8
-0.6
-0.4
-0.2
0
0.2
90
90.5
91
91.5
92
92.5
93
Temperature (K)
Ho
Dy

Figure 9

Fig. 10

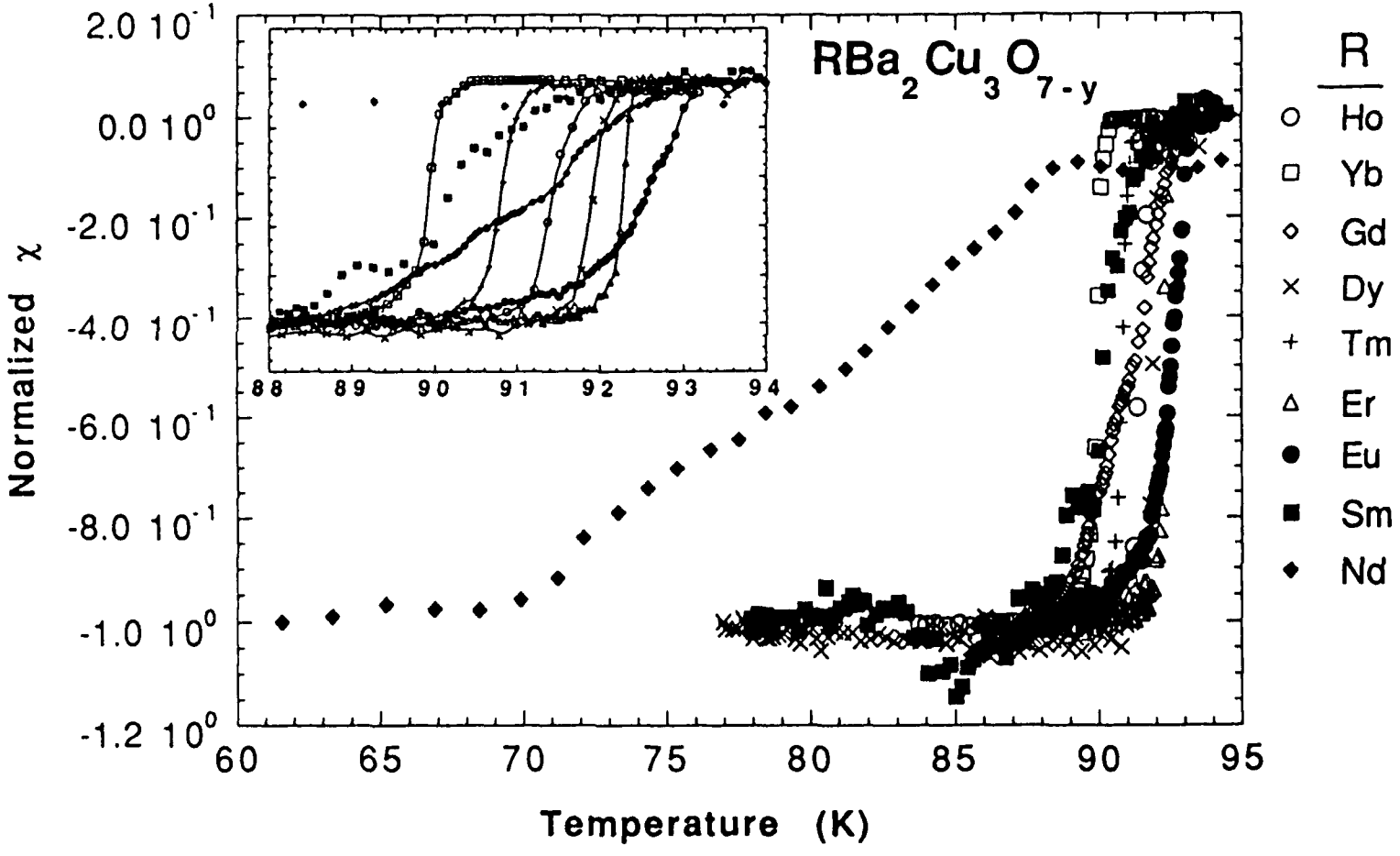
RBa2Cu3O7-y
Normalized χ
Temperature (K)
2.0 10-1
0.0 10^0
-2.0 10-1
-4.0 10-1
-6.0 10-1
-8.0 10-1
-1.0 10^0
-1.2 10^0
60
65
70
75
80
85
90
95
88
89
90
91
92
93
94
R
Ho
Yb
Gd
Dy
Tm
Er
Eu
Sm
Nd

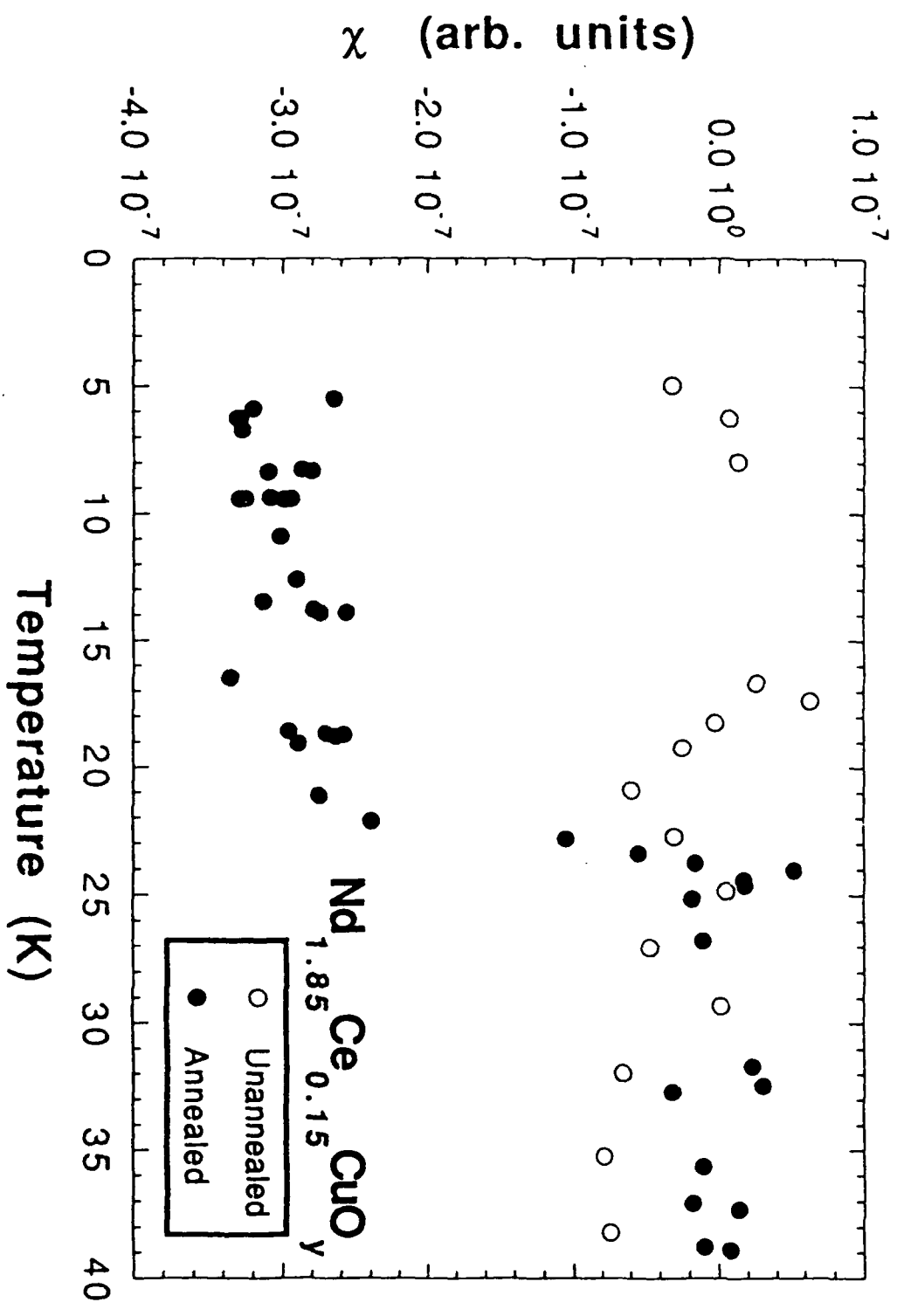
χ (arb. units)
1.0 10⁻⁷
0.0 10⁰
-1.0 10⁻⁷
-2.0 10⁻⁷
-3.0 10⁻⁷
-4.0 10⁻⁷
0
5
10
15
20
25
30
35
40
Temperature (K)
Nd1.85Ce0.15CuOy
Unannealed
Annealed

Figure 11